PVDIS GEM BACKGROUNDS FROM GEM COPPER

R. HOLMES

1. Introduction

Optimization of the thickness of the GEM planes has been a subject of ongoing investigation. In particular, the copper layers of the cathode, GEM foils, and readout planes are potentially a significant background source. This report discusses GEM thickness and contributions of GEM copper to PVDIS background rates and strip occupancies.

2. Copper in GEMs

PVDIS backgrounds in the GEMs are due mainly to photons interacting in the GEMs or elsewhere, producing electrons (and positrons) that deposit energy in the GEMs. These electrons can be produced externally to the GEMs they produce signals in. They also can be produced internally.

A particular concern is low energy photons which produce low energy electrons in a GEM; these electrons then deposit most or all of their energy in the drift layer, giving rise to a large charge deposition over a relatively large number of strips. Such low energy tracks can make a disproportionately large contribution to strip occupancy.

Table 1 gives thicknesses for the various layers of a triple GEM detector similar to what is implemented in our present simulation. The total thickness is 0.41% of a radiation length (X_0) of which 0.24% is copper.

R&D has been done on a copper free GEM foil, in which the copper layer from a standard GEM foil is removed leaving a 100 nm chromium conductive layer.[1] Thickness comparisons between a standard GEM plane and one with no copper layers have been shown; such a completely copper free GEM would be less than half as many radiation lengths in thickness as a standard GEM. In reality, at PVDIS exposure rates it is expected that, at best, only the first two GEM layers can be copper free without suffering unacceptable damage. Further research will be required to explore this possibility.

More recently, an alternative to the GEM design has been studied. The μRWELL design uses a single foil in place of the three GEM foils.[2] Potential benefits include both cost savings and thickness reduction, although the resistive readout limits rate to about 100 kHz/cm^2 to date.

Table 2 shows a breakdown of layer thicknesses for a μRWELL detector similar to the prototype studied at UVA. The total thickness, $0.37\%X_0$, and total copper thickness, $0.21\%X_0$, are not much less than what is shown in Table 1 for the standard GEMs. The reason is mainly due to the much thicker copper layers in the readout.

TABLE 1. Thicknesses of layers in a triple GEM plane similar to what is implemented in our present simulation.

Layer	Material	Thickness (μm)	Area fraction	$\%X_0$
Window	Aluminum	5	1	0.0056
	Kapton	25	1	0.0087
Gas gap	ArCO2	3000	1	0.0015
Cathode	Kapton	50	1	0.0175
	Copper	5	1	0.0348
Gas gap	ArCO2	3000	1	0.0015
Foil 1	Copper	5	0.8	0.0279
	Kapton	50	0.8	0.0140
	Copper	5	0.8	0.0279
Gas gap	ArCO2	2000	1	0.0010
Grid spacer	G10	2000	0.0082	
Foil 2	Copper	5	0.8	0.0279
	Kapton	50	0.8	0.0140
	Copper	5	0.8	0.0279
Gas gap	ArCO2	2000	1	0.0010
Grid spacer	G10	2000	0.0082	
Foil 3	Copper	5	0.8	0.0279
	Kapton	50	0.8	0.0140
	Copper	5	0.8	0.0279
Gas gap	ArCO2	2000	1	0.0010
Grid spacer	G10	2000	0.0082	
Readout U	Copper	5	0.2	0.0070
	Kapton	50	0.2	0.0035
Readout V	Copper	5	0.75	0.0261
	Kapton	50	1	0.0175
	Glue	60	1	0.0300
Gas gap	ArCO2	3000	1	0.0015
Window	Kapton	25	1	0.0087
	Aluminum	5	1	0.0056
Total				0.4066
Total Cu				0.2350

Part of the reason for the increased thickness is simply that this was a prototype for testing and the thickness was not a major concern. Per discussions with Kondo, these layers could be made thinner. However, to accommodate our readout requirements, vias holes will have to be provided in the readout layers, and this necessitates thicker copper than would otherwise be possible. Thicknesses of about 12μm rather than 25μm are probably usable. However, Kondo also points out *the same thickness requirements would apply to*

TABLE 2. Thicknesses of layers in a μRWELL plane similar to the prototype studied at UVA.

Layer	Material	Thickness (μm)	Area fraction	$\%X_0$
Window	Aluminum	2	1	0.0022
	Kapton	25	1	0.0087
Gas gap	ArCO2	3000	1	0.0015
Cathode	Kapton	25	1	0.0087
	Aluminum	2	1	0.0022
Gas gap	ArCO2	3000	1	0.0015
Foil 1	Copper	5	0.8	0.0279
	Kapton	50	0.8	0.0140
	DLC	0.1	1.0	0.0000
	G10	50	1.0	0.0258
Readout U	Copper	25	0.2	0.0348
	G10	50	0.2	0.0035
Readout V	Copper	25	0.85	0.1480
	G10	100	1.0	0.0515
Gas gap	ArCO2	3000	1	0.0015
Window	Kapton	25	1	0.0087
	Aluminum	2	1	0.0022
Total				0.365
Total Cu				0.211

the GEM readout layers as well. That is, the 5μm thicknesses we have been assuming probably are too small.

What emerges from this discussion is that it is too early to know what thickness is realistic for our tracking detectors. Further R&D will be required to determine how much copper will be necessary, and the importance of that effort will be driven by our understanding of the effects of this material.

3. Fluxes from GEM layers

Our GEMC Monte Carlo output files do not contain information linking external tracks to internal energy-depositing hits in the GEMs. However, we can look in the virtual flux detectors in front of the GEMs for hits closest to the energy depositions and then plot the vertex coordinates associated with those flux detector hits. Figure 1 top left shows the radial vertex coordinate versus the z vertex coordinate for photon hits in the GEM3 flux detector associated with energy deposition, from a simulation of 10^9 electrons on target and the standard PVDIS apparatus; the top right scatterplot is the same for electron hits. Below these are corresponding histograms of vertex z, with the vertical axes scaled to the flux per sector in MHz. The target, baffles, and downstream material including GEMs 1 to 3 are evident. Figure 2 shows zoomed-in views around GEM 1 (left) and GEMs 2–3

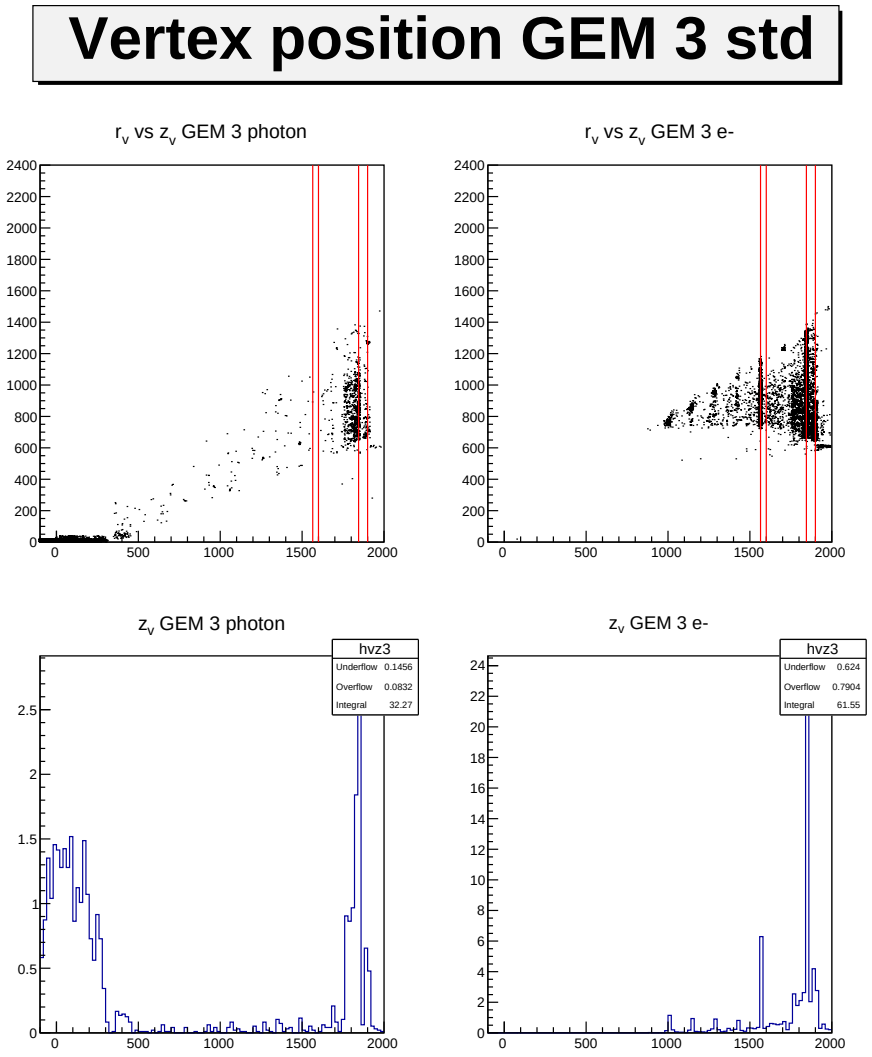

FIGURE 1. Top: Scatterplot of vertex r coordinate (in mm) vs. vertex z coordinate (in mm) for photon (left) or electron (right) tracks hitting the GEM 3 flux detector and associated with nearby energy deposition in GEM 3, for standard beam on target Monte Carlo data. Red lines indicate z bounds of GEM 1 (near $z = 1600$ mm) and GEMs 2 and 3 (near $z = 1850$ mm). Bottom: Histogram of vertex z coordinate (in mm) for photon (left) or electron (right) tracks hitting the GEM 3 flux detector and associated with nearby energy deposition in GEM 3. Vertical axis is flux in MHz per sector.

(right) for photon tracks, and Fig. 3 is similar but for electrons. The copper-Kapton layer structure of the GEMs is evident, demonstrating that backgrounds in GEM 3 can come from interactions in the material layers of that GEM as well as GEM 2 and, to a lesser degree, GEM 1. The integrated fluxes for all vertex positions and for vertexes in or near the upstream GEMs are shown in Table 3 (for photon tracks) and Table 4 (for electron tracks).

TABLE 3. Fluxes at GEMs for background-associated photon tracks, from all vertex positions and from vertexes in or near the GEMs, from standard Monte Carlo.

GEM	Flux (all z; MHz/sector)	Flux for z near GEM 1	Flux for z near GEMs 2–3	Flux for z near GEMs 4–5
1	102.7	2.6	0.1	
2	46.3	0.0	1.2	
3	32.3	0.0	1.6	
4	17.7	0.0	0.1	0.4
5	16.4	0.0	0.0	1.5

TABLE 4. Fluxes at GEMs for background-associated electron tracks, from all vertex positions and from vertexes in or near the GEMs, from standard Monte Carlo.

GEM	Flux (all z; MHz/sector)	Flux for z near GEM 1	Flux for z near GEMs 2–3	Flux for z near GEMs 4–5
1	149.7	13.3	1.5	
2	84.9	17.9	9.6	
3	61.1	6.0	25.7	
4	34.7	0.1	0.2	3.6
5	40.1	0.0	0.2	17.8

Tables 5 and 6 are similar, but for Monte Carlo data in which the copper in the GEMs is replaced by ArCO2 gas. This data set is an order of magnitude smaller (10^8 electrons on target) than the standard one. There is little change in the electron flux but the photon flux is reduced by about 30%.

4. Energy deposition

Different energy tracks produce different responses in the GEMs. The top left plot in Fig. 4 shows $\log(E_{dep}/(1\text{ MeV}))$ versus $\log(p/(1\text{ MeV}))$ for background-associated photon hits in the GEM 1 flux detector, where E_{dep} is the energy deposited in the GEM close to the photon position and p is the photon momentum. There are two populations of photons, with p in the range about 10 to 100 keV and in the range about 300 keV and up.

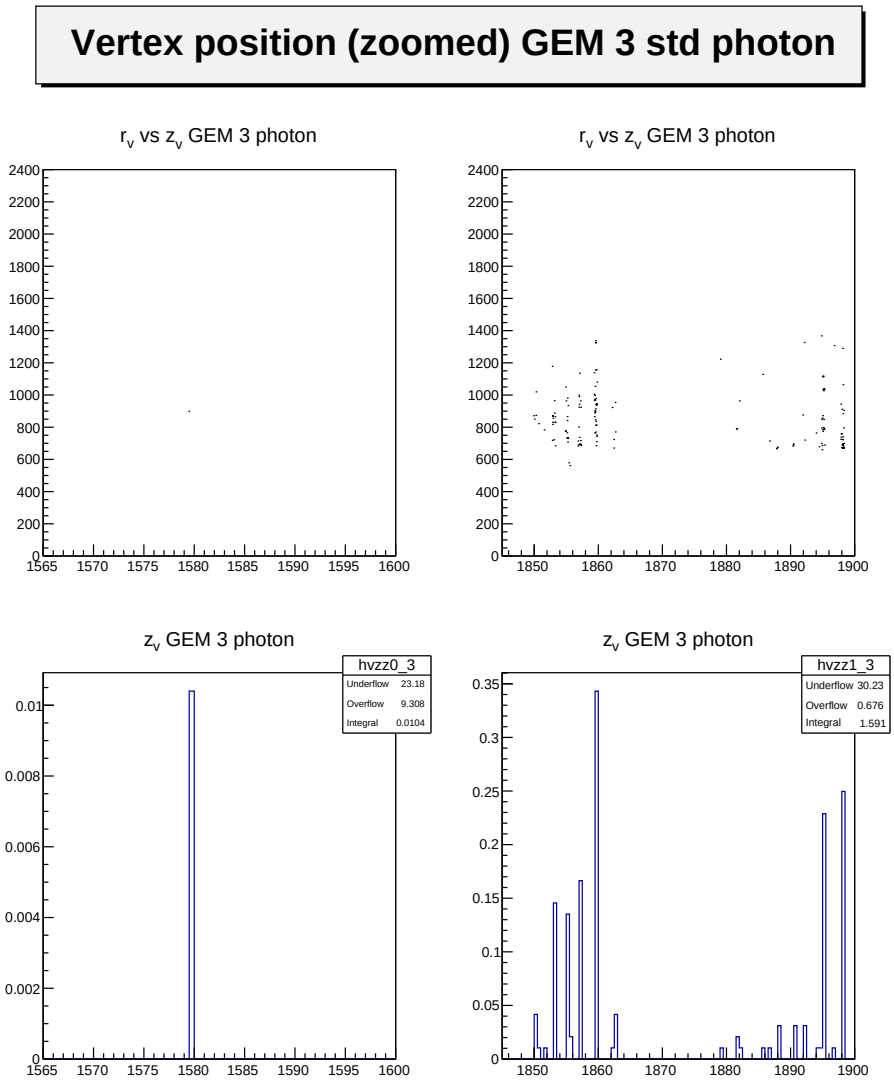

FIGURE 2. Top: Scatterplot of vertex r coordinate (in mm) vs. vertex z coordinate (in mm) for photon tracks hitting the GEM 3 flux detector and associated with nearby energy deposition in GEM 3, zoomed in on z near GEM 1 (left) and GEMs 2 and 3 (right), for standard Monte Carlo data. Bottom: Histogram of vertex z coordinate (in mm) for photon tracks hitting the GEM 3 flux detector and associated with nearby energy deposition in GEM 3, zoomed in on z near GEM 1 (left) and GEMs 2 and 3 (right). Vertical axis is flux in MHz per sector.

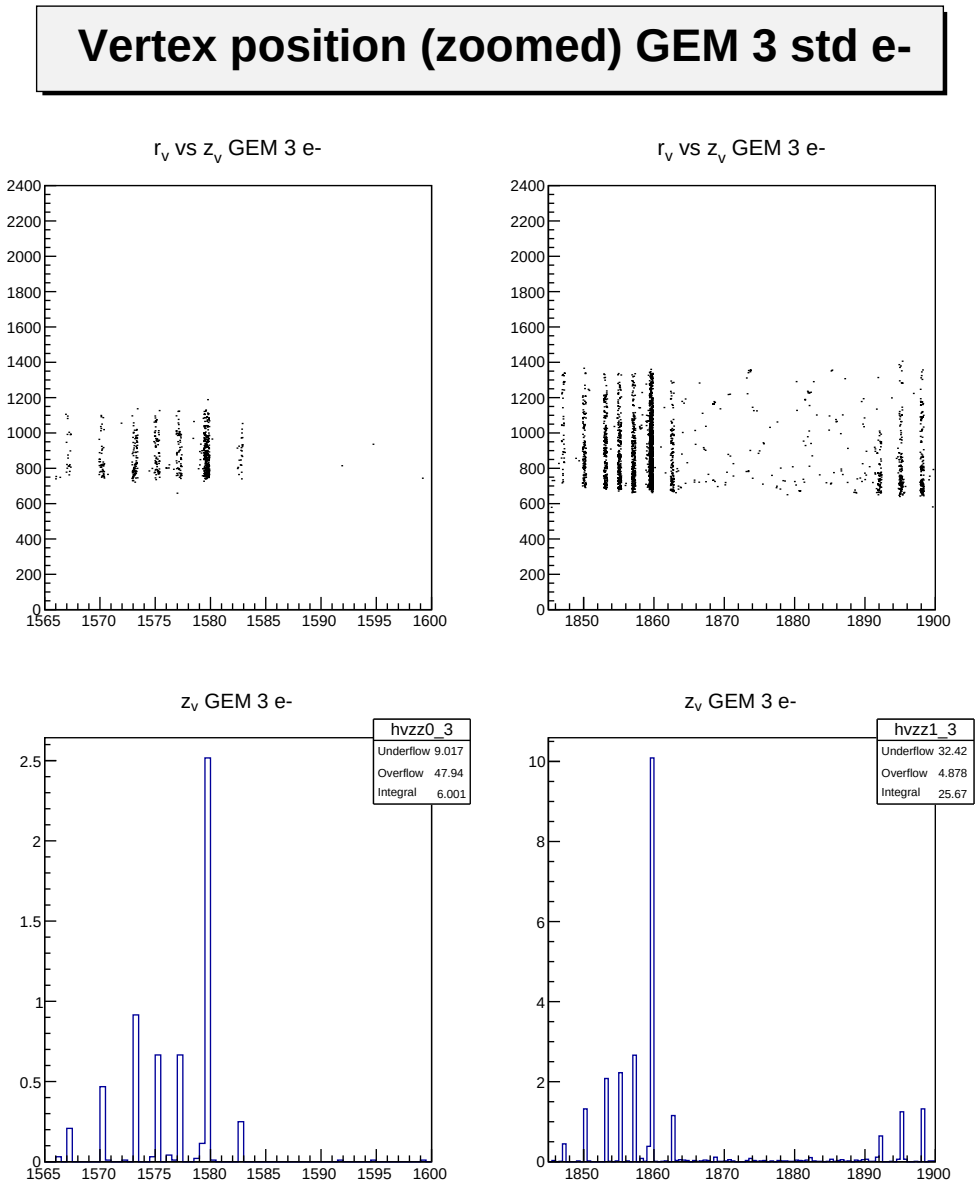

FIGURE 3. Similar to Fig. 2, but for electron tracks.

TABLE 5. Similar to Table 3, but for a simulation where GEM copper is replaced by ArCO2 gas.

GEM	Flux (all z; MHz/sector)	Flux for z near GEM 1	Flux for z near GEMs 2–3	Flux for z near GEMs 4–5
1	66.5	1.9	0.0	
2	34.9	0.0	0.1	
3	22.4	0.0	4.1	
4	10.0	0.0	0.1	0.4
5	11.5	0.0	0.1	1.2

TABLE 6. Similar to Table 4, but for a simulation where GEM copper is replaced by ArCO2 gas.

GEM	Flux (all z; MHz/sector)	Flux for z near GEM 1	Flux for z near GEMs 2–3	Flux for z near GEMs 4–5
1	168.7	9.9	1.52	
2	79.9	13.4	8.6	
3	61.5	5.7	22.1	
4	37.0	0.0	0.1	3.6
5	44.0	0.0	0.1	17.3

Middle left is the distribution of $\log(E_{dep}/(1\text{ MeV}))$ for these photon hits, for all photons (dark blue), lower (< 100 MeV) momentum photons (light blue), and higher (> 100 MeV) momentum photons (red). There is typically an order of magnitude more energy deposited by the lower momentum photons.

As seen on the right in the same figure, there is no similar structure in the electrons. Essentially all have $p > 100$ MeV and are minimum ionizing.

The bottom left plot shows the distribution of the *total* energy deposition over the entire GEM in an event, for all events (dark blue), events where the minimum photon momentum is lower than 100 MeV (light blue), and events where the minimum photon momentum is higher than 100 MeV (red). Events having a low momentum photon peak at much higher E_{dep} than those that do not, producing a shoulder in the total distribution. Similar behavior is seen in all GEMs.

Figure 5 is similar but for the no-copper simulation. Bearing the reduced statistics in mind, the low-p, high-E_{dep} photon component is much reduced relative to the rest. There is little or no shoulder evident in the whole-GEM E_{dep} distribution.

5. OCCUPANCY

The significance of the high-E_{dep} events is that larger energy deposition can be expected to put more charge on the strips, sending larger numbers of strips above threshold. This expectation has been verified in Monte Carlo studies by Weizhi. High-E_{dep} events could

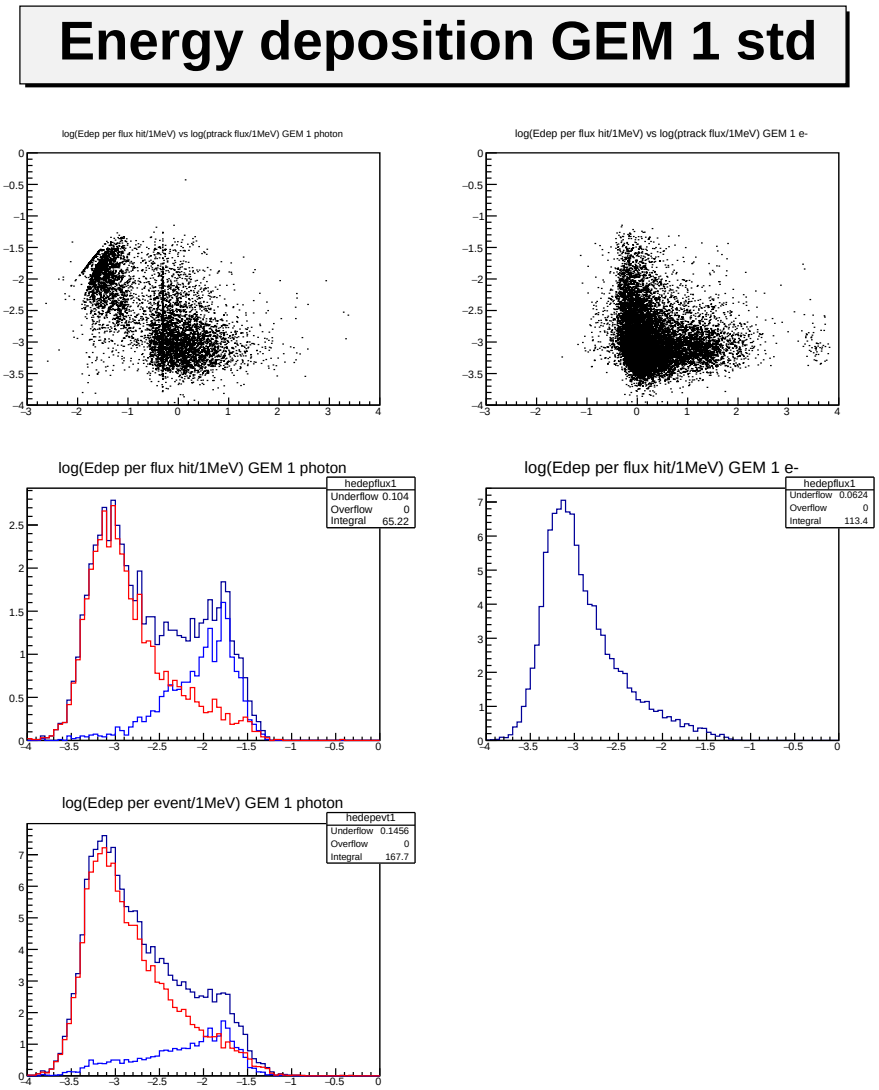

FIGURE 4. Top left: Scatterplot of log of energy deposition in GEM 1 near a photon track hitting the GEM 1 flux detector vs. log of photon momentum, for standard Monte Carlo data. Middle left: Distribution of log of energy deposition. Top and middle right: Similar but for electron tracks. Bottom left: Distribution of energy deposition in the entire GEM. See text for details.

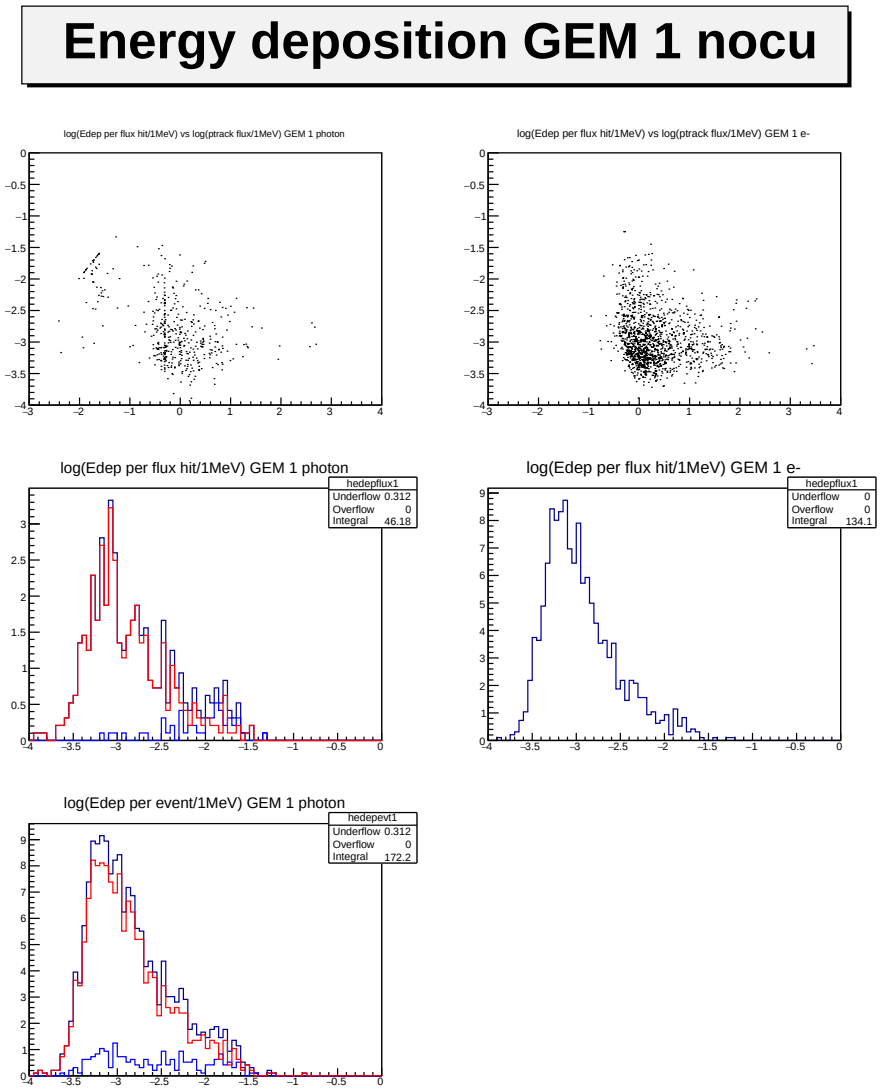

FIGURE 5. Similar to Fig. 4, but for a simulation where GEM copper is replaced by ArCO2 gas.

therefore increase strip occupancy, defined for each strip as the fraction of events where that strip is above threshold.

To examine this effect, occupancies for three simulations were studied: our standard Monte Carlo, the Monte Carlo with GEM copper replaced by ArCO2, and a Monte Carlo with the standard GEMs but with tracks having kinetic energy below 100 keV discarded.

The strips were not divided and there were no high voltage dead regions. These occupancies are shown in Fig. 6. The small sizes of the latter two data sets limits the precision of

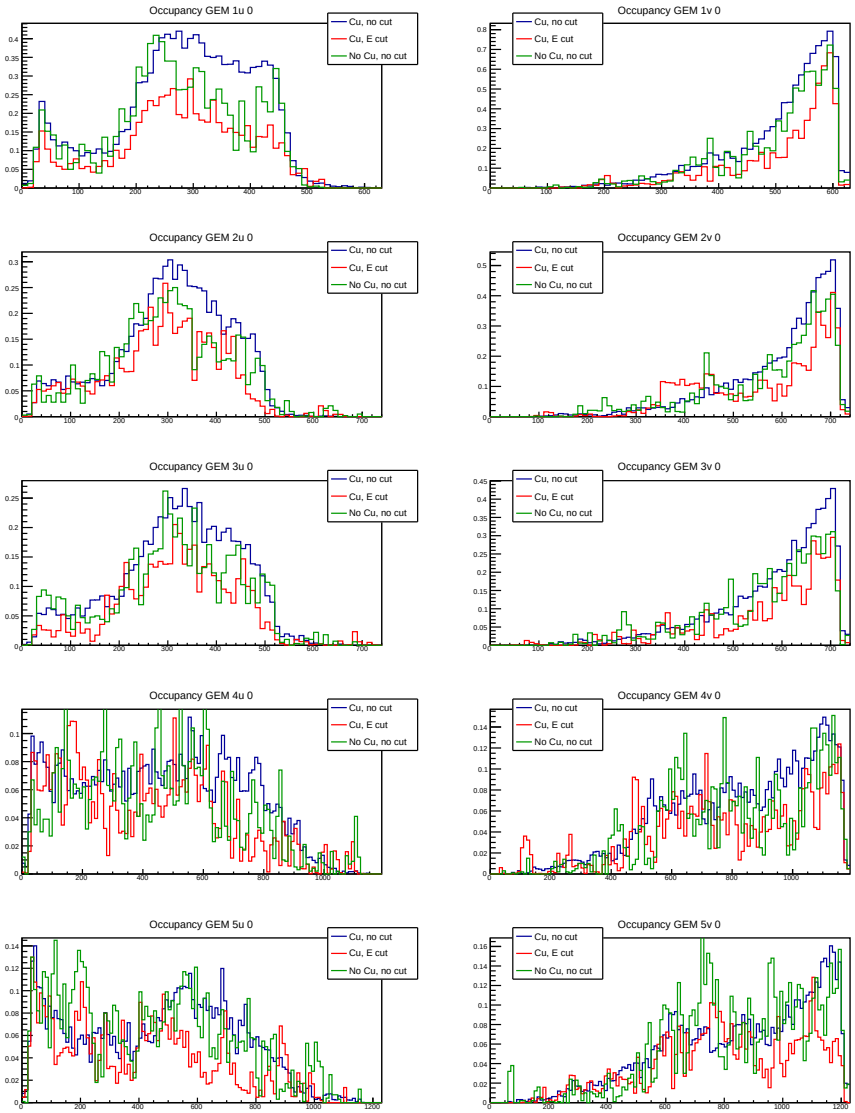

FIGURE 6. Occupancies for GEMs 1 through 5 (rows), U and V strips (columns), for three data sets: Standard (blue), standard GEMs with tracks having < 100 keV kinetic energy discarded (red), and GEMs with copper replaced by ArCO2 (green).

these distributions, but it is evident complete elimination of low-energy tracks reduces the

occupancies in the U strips of GEM 1 by about 40%. A smaller reduction, about 25%, results from eliminating the copper. The effects are smaller in GEMs 2 and 3 and not evident in GEMs 4 and 5.

The V strips of GEM 1 are where we see the largest occupancies, approaching 80% along the high edge. This peak occupancy is not reduced much by the energy cut or copper elimination. When the flux is sufficiently high to make the occupancy approach 100%, even a large flux reduction may not greatly reduce the likelihood of hitting a strip in an event, so the occupancy stays high.[1] Away from the peak in GEM 1 V, the occupancy reduction is similar to what is generally seen in the U strips.

We see that reducing the amount of copper in the GEMs can reduce occupancy, but even the complete elimination of copper does not do much to lower the peak occupancy upstream, and away from the peak the occupancy reduction is much less than a factor of 2. More realistic levels of copper reduction would likely improve occupancies by only something on the order of 10%.

References

[1] K. Gnavo, "Status of GEM-US @ UVA", SoLID Collaboration meeting, 15 May 2015
[2] N. Liyanage, "GEM detectors for SoLID", SoLID Collaboration meeting, 8 Jun 2018

[1]That is, in a model where the hits on a strip are uncorrelated and the number of hits can be described by a Poisson distribution $P(n;\mu)$, where μ is the expected number of hits per event, the occupancy is just $O(\mu) = 1 - P(0;\mu) = 1 - e^{-\mu}$ and the change in occupancy with μ is $dO(\mu) = e^{-\mu}d\mu = (1 - O(\mu))d\mu$. Then for example if the occupancy is 50%, $dO = 0.5d\mu$, but when $O = 80\%$, $dO = 0.2d\mu$. The higher the occupancy, the less responsive it is to changes in hit rates.